Journal Pre-proof

Design and synthesis of novel bis-pyridinium based-ionic liquids as potent antiparasitic agents

Esraa Abdelhamid Moneer, Basant A. Bakr, Sara H. Akl, Yahya H. Shahin, Bassma H. Elwakil, Mohamed Hagar, Keshav Raj Paudel, Ateyatallah Aljuhani, Mohamed Reda Aouad, Nadjet Rezki

Please cite this article as: , Design and synthesis of novel bis-pyridinium based-ionic liquids as potent antiparasitic agents, *HELIYON* (2023), doi: https://doi.org/10.1016/j.heliyon.2023.e15431.

Design and synthesis of novel bis-pyridinium based-ionic liquids as potent antiparasitic agents

Esraa Abdelhamid Moneer[1], Basant A. Bakr[2], Sara H. Akl[1], Yahya H. Shahin[1], Bassma H. Elwakil[1,*], Mohamed Hagar[3], Keshav Raj Paudel[4], Ateyatallah Aljuhani[5], Mohamed Reda Aouad[5], Nadjet Rezki[5]

[1]Department of Medical Laboratory Technology, Faculty of Applied Health Sciences Technology, Pharos University in Alexandria, Alexandria, Egypt

[2]Department of Zoology, Faculty of Science, Alexandria University, Alexandria 21321, Egypt

[3]Department of Chemistry, Faculty of Science, Alexandria University, Alexandria 21321, Egypt

[4]Department of Oriental Medicine Resources, Mokpo National University, Muan-gun, Jeonnam 58554, Republic of Korea

[5]Department of Chemistry, College of Science, Taibah University, Al-Madinah Al-Munawarah 30002, Saudi Arabia

*Correspondence: Bassma.hassan@pua.edu.eg (B.H.E)

Abstract

Focused bis-pyridinium based-ionic liquids were successfully synthesized through the quaternization of the selected 1,2-di(pyridin-4-yl)ethane followed by metathetical anion exchange. The synthesized pyridinium derivatives were fully characterized using various NMR-spectroscopic techniques including ^{1}H, ^{13}C, ^{11}B, ^{31}P and ^{19}F-NMR. The synthesized compounds were tested for their potential effect against *Toxoplasma gondii*. It was revealed that compound 5 had higher antiparasitic activity compared to other compounds. Parasitic reduction percentage reached 38, 50, 77 and 79 for groups III, IV, V and VI respectively in the liver with noticed distortion and deformation in tachyzoites' shape. Surprisingly there was no statistically significant difference between the synthesized compound 5 and the known anti-toxoplasmosis drug pyrimethamine. Histopathological study proved the effectiveness of the synthesized compound 5 on liver, spleen and brain tissues with observed better histological features compared to pyrimethamine treated group. The present investigation may pave the way to the possible use of compound 5 to replace the known drug pyrimethamine with better antiparasitic profile and fewer side effects.

Keywords: Ionic Liquids; Dicationic ionic liquids; toxoplasmosis infections; antiparasitic agents

1. Introduction

For many years, ionic liquids (ILs), which are essentially 'liquid salts' based on organic and/or inorganic ions and may encompass more than one cation or anion, were known as salts that melt at temperatures around 100 °C [1, 2] These are common class of bis-ionic liquids (bis-ILs) that contain a bis-cations and two identical anions, known as di-cationic ionic liquids, and have emerged as an intriguing and entertaining modern material in technology and science due to their broad range of uses in a variety of fields [3]. The chemistry of ILs has recently get to be a contentious issue, as it is critical in the design and build out of modern scaffolds, along with understanding their biological benefits and attributes that aid in their development and synthesis [1, 4, 5]. These tunable molecules are well known for their high stability and safety properties, which include nonvolatility and nonflammability, negligible vapor pressure, thermal stability and

45 high ionic conductivity, easy recyclability, and high miscibility in both organic and aqueous

46 solvents. They are easily designed and constructed by combining bulky organic cations with

47 either inorganic or organic anions to achieve the desired structural frameworks with focused

48 characteristics like melting point, lower toxicity, and density, as well as continuing to increase

49 benefits in biological implantation [6-12].

50 Toxoplasmosis is a zoonotic infection that causes a distinct health problem in humans, wildlife,

51 and domestic animals. It can infect animals and humans in any ecosystem, including food, soil,

52 and water [13]. *Toxoplasma gondii* is considered among the most widely distributed parasites.

53 Nearly one-third of the world's population was exposed to *T. gondii* through contaminated food

54 and water, especially in areas with poor sanitation [14]. It is also considered a global health risk

55 due to its high global seroprevalence, which varies with various regional differences in hygiene,

56 diet, habits, climate, and host susceptibility [15].

57 It has been reported that *T. gondii* spreads by three main routes, the first is by eating oocysts in

58 contaminated water, soil, or food; the second is by ingesting cysts from infected animal tissues; it

59 is due to vertical transmission from HIV to the fetus [13]. Infection is usually considered

60 asymptomatic if it has no symptoms. Primary infections can harm the fetus during pregnancy and

61 even lead to abortion. Moreover, in immunocompromised humans and animals, primary parasitic

62 infection or relapse can lead to severe neurological clinical manifestations, with implications for

63 public health and animal production [16]. When infection first begins, *T. gondii* spreads to

64 mesenteric lymph nodes before invading blood and lymphatic vessels to spread to other organ

65 systems. The parasite can then grow almost anywhere in the body's cells. Similar to many other

66 common explicitly require intracellular pathogenic microbes, *T. gondii* infection triggers a type 1

67 polar immune response that targets both innate and adaptive immunity [13]. It is well recognized

68 that the production of pro-inflammatory cytokines interferes with the host's main defense

69 mechanism against toxoplasmosis [17]. Tachyzoite replication is squelched by the host's T-cell

70 mediated immune responses, which may result in chronic infection or parasite clearance [18].

71 Since 1950, sulfadiazine and pyrimethamine have been used in combination to treat human

72 toxoplasmosis infections. Through simultaneous inhibition of the enzymes dihydrofolate

73 reductase and dihydropteroate synthase, these medications work to prevent the synthesis of folate

74 (essential enzymes for parasite replication and survival) [19, 20]. Although, Sulfadiazine exhibits

75 many side effects and might lead to megaloblastic anemia, granulocytopenia and leukopenia

76   [19]. Besides that, pyrimethamine is highly harmful because it encounters the host's and

77   parasite's biochemical pathways in overall [21].

78   These attributes have improved dramatically our both functional and structural experience and

79   knowledge as part of our current advancement for the development of powerful and effective

80   ionic liquids framework carrying di-pyridinium ionic liquids [22-25]. Many research groups have

81   engaged in a broad array of novel chemical development against *T. gondii* to find anti-

82   toxoplasmosis drugs that are extremely effective and have minimal risky side effects. Thus, in

83   this study, we have anticipated to design, synthesize and characterize focused bis-pyridinium

84   ionic liquids encompassing benzyl side chains and different counter-anions. Furthermore, we

85   investigated the antiparasitic properties of the synthesized bis-ILs against Toxoplasmosis,

86   establishing their reduction activity. Premised on a thorough literature review, this study is the

87   first to investigate the potential of bis-ILs to attenuate the anti-*T. gondii* infection.

88   **2. Experimental**

89   *2.1. Chemistry*

90   *2.1.1. General methods*

91   The melting points were measured using a Stuart Scientific SMP1 instrument and are

92   uncorrected. The characterization of the newly designed bis-pyridinium ionic liquids has been

93   achieved by IR, ^{1}H, ^{13}C, ^{19}F, ^{31}P, ^{11}B-NMR spectroscopy and elemental analysis. The 500 MHz

94   Jeol NMR spectrometer was used to elaborate all NMR spectra. Elemental analyzes were

95   performed using a GmbH-Vario EL III Elemental Analyzer.

96   **Synthesis and characterization of 4,4'-(ethane-1,2-diyl)bis(1-benzylpyridin-1-ium) bromide**

97   **(2)**

98   Under stirring, benzyl bromide (20 mmol) was drop-wisely added to 1,2-di(pyridin-4-yl)ethane

99   (**1**) solution (20 mmol) in acetonitrile (40 mL). TLC showed that the starting material had been

100 consumed after 16 hours heating under reflux. Evaporation under reduced pressure was used to

101 reduce the solvent. The resulting product was filtered to yield the desired di-cationic pyridinium

102 ionic liquid **2**.

103 Yield: 94%; mp: 35-36 °C. IR (v, cm^{-1}): 3052 (Sp^{2}C-H), 2988 (Sp^{3}C-H), 1630 (C=N), 1564

104 (C=C).^{1}H-NMR (DMSO-d_6, 400 MHz): δ_H = 9.18 (2H, s, Pyridyl-**H**), 8.14 (2H, s, Pyridyl-**H**),

105   7.50 (2H, s, Ph-**H**), 7.34 (3H, d, J = 4.0 Hz, Ph-**H**), 5.83 (2H, s, NC**H**$_2$), 3.23 (2H, s, CH$_2$C**H**$_2$).

106   ^{13}C-NMR (DMSO-d_6, 100 MHz): δ_C = 161.22, 144.70, 134.90, 129.85, 129.72, 129.29, 128.73

107   (**C**=N, Ar-**C**); 62.83 (N**C**H$_2$); 34.28 (CH$_2$**C**H$_2$). Calculated for C$_{26}$H$_{26}$Br$_2$N$_2$: C, 59.33; H, 4.98;

108   N, 5.32. Found: C, 59.56; H, 4.87; N, 5.49.

109   General metathesis procedure for the synthesis of bis-benzyl pyridinium based-ionic

110   liquids 3-5

111   A stirred suspension of compound **2** (1 mmol) in acetonitrile (20 mL) containing the

112   corresponding potassium hexafluorophosphate, sodium tetrafluoroborate, and/or sodium

113   thiocyanate (2.2 mmol) was refluxed for 24 hours. After the mixture cooling, the resulting crude

114   product was collected using filtration, which was then washed with acetonitrile, left to dry and

115   crystallized from ethanol yielding the targeted dicationic bis-pyridinium derivatives **3-5**.

116   Characterization of 4,4'-(ethane-1,2-diyl)bis(1-benzylpyridin-1-ium) hexafluorophosphate

117   (3)

118   Yield: 90%; syrup. IR (v, cm^{-1}): 3047 (Sp^{2}C-H), 2997 (Sp^{3}C-H), 1636 (C=N), 1570 (C=C).^{1}H-

119   NMR (DMSO-d_6, 400 MHz): δ_H = 9.16 (2H, s, Pyridyl-**H**), 8.11 (2H, s, Pyridyl-**H**), 7.51 (2H, s,

120   Ph-**H**),7.36 (3H, d, J = 4.0 Hz, Ph-**H**), 5.82 (2H, s, NC**H**$_2$), 3.27 (2H, s, CH$_2$C**H**$_2$). ^{13}C-NMR

121   (DMSO-d_6, 400 MHz): δ_C = 161.20, 144.67, 134.91, 129.85, 129.89, 129.31, 128.69 (**C**=N, Ar-

122   **C**); 62.86 (N**C**H$_2$); 34.30 (CH$_2$**C**H$_2$). ^{31}P-NMR (DMSO-d_6, 162 MHz) δ_P =-131.01 to-157.36

123   (1P, sept, **P**F$_6$). ^{19}F NMR (DMSO-d_6, 377 MHz): δ_F = -69.25 (6F, d, P**F$_6$**). Calculated for

124   C$_{26}$H$_{26}$F$_{12}$N$_2$P$_2$: C, 47.57; H, 3.99; N, 4.27. Found: C, 47.30; H, 3.88; N, 4.44.

125   Characterization of 4,4'-(ethane-1,2-diyl)bis(1-benzylpyridin-1-ium) tetrafluoroborate (4)

126   Yield: 92%; syrup. IR (v, cm^{-1}): 3049 (Sp^{2}C-H), 2999 (Sp^{3}C-H), 1638 (C=N), 1573 (C=C).^{1}H-

127   NMR (DMSO-d_6, 400 MHz): δ_H = 9.10 (2H, d, J = 4.0 Hz, Pyridyl-**H**), 8.07(2H, d, J = 4.0 Hz,

128   Pyridyl-**H**), 7.48-7.39 (5H, m, Ph-**H**), 5.76 (2H, s, NC**H**$_2$), 3.27 (2H, s, CH$_2$C**H**$_2$). ^{13}C-NMR

129   (DMSO-d_6, 100 MHz): δ_C = 161.10, 144.83, 134.95, 129.88, 129.78, 129.21, 128.66 (**C**=N, Ar-

130   **C**); 63.22 (N**C**H$_2$); 34.27 (CH$_2$**C**H$_2$). ^{11}B-NMR (DMSO-d_6, 128 MHz): δ_B = -1.28 to -1.30 (1B,

131   m, **B**F$_4$). ^{19}F-NMR (DMSO-d_6, 377 MHz): δ_F = -148.24, -148.31 (4F, 2d, B**F**$_4$). Calculated for

132   C$_{26}$H$_{26}$B$_2$F$_8$N$_2$: C, 57.82; H, 4.85; N, 5.19. Found: C, 57.61; H, 4.95; N, 5.32.

133   Characterization of 4,4'-(ethane-1,2-diyl)bis(1-benzylpyridin-1-ium) thiocyanate (5)

134 Yield: 90%; mp: 47-48 °C. IR (v, cm^{-1}): 3043 (Sp^{2}C-H), 2980 (Sp^{3}C-H), 2064 (SCN), 1634

135 (C=N), 1570 (C=C). ^{1}H-NMR (DMSO-d_6, 400 MHz): δ_H = 9.21 (2H, s, Pyridyl-**H**), 8.15 (2H, s,

136 Pyridyl-**H**), 7.53 (2H, s, Ph-**H**), 7.38 (3H, s, Ph-**H**), 5.85 (2H, s, NC**H**$_2$), 3.29 (2H, s, CH$_2$C**H**$_2$).

137 ^{13}C-NMR (DMSO-d_6, 100 MHz): δ_C = 161.22, 144.79, 134.96, 129.87, 129.76, 129.26, 128.69

138 (**C**=N, Ar-**C**); 63.10 (N**C**H$_2$); 34.29 (**C**H$_2$CH$_2$). Calculated for C$_{28}$H$_{26}$N$_4$S$_2$: C, 69.68; H, 5.43; N,

139 11.61. Found: C, 69.85; H, 5.36; N, 11.73.

2.2. Cytotoxicity test

141 Cytotoxicity test was determined in a liver cell line (HepG2). 100 units/mL of penicillin and 100

142 mg/mL of streptomycin were added to DMEM medium (supplemented with 10% FBS) to grow

143 the normal liver cells which were maintained in 5% CO$_2$ at 37 °C. Then two-fold serially diluted

144 concentrations of each tested compound were prepared. Confluent monolayers of normal liver

145 cells were grown in 96-well microtiter plates for 24 h then the prepared concentrations were

146 added to the grown cells then furtherly incubated for 72 h. After the incubation period, 20 μL

147 MTT (5 mg/mL) was added to each well, incubated at 37 °C for 4 h. The optical density (OD)

148 was measured at 570 nm and the cytotoxic concentration (CC$_{50}$), was estimated from graphic

149 plots of the dose response curve for each tested concentration [26].

Parasite

151 The virulent strain *T. gondii* RH was supplied from the Parasitology Laboratory of Theodor

152 Bilharz Research Institute, Giza, Egypt. The parasite was kept alive at Pharos University

153 (Alexandria) by serial intraperitoneal passages of tachyzoites in Swiss albino mice. Peritoneal

154 fluid was washed using phosphate-buffered saline (PBS). A drop of the collected peritoneal

155 exudate was counted using hemocytometer and mice were infected with specified number of

156 tachyzoites (2500 tachyzoites/100 μL).

2.2.1. Drugs preparation

158 The tested Di-ILs **2, 4** and **5** were suspended in saline (100 μL) and orally administered as a

159 single dose/mouse for 7 days starting from the day of infection.

2.2.2. Animal grouping and experimental design

161 The study here included 60 BALB/c male mice (6–8 weeks old) weighing between 20 to 25 g.

162 Mice were divided into 6 groups (10 mice/group) in which each mouse was assigned to specified

163 treatment regimen (received via oral gavage needle starting from the day of infection) as
164 following:

165 **Group I**: Healthy control group (received 100 μL saline for 7 days).

166 **Group II**: Infected untreated control group (received 100 μL of saline for 7 days).

167 **Group III:** Infected, compound **2** treated group (received 100 μL of compound **2** at a dose of
168 12.5 mg/kg/day for 7 days).

169 **Group IV**: Infected, compound **4** treated group (received 100 μL of compound **4** at a dose of
170 12.5 mg/kg/day for 7 days).

171 **Group V**: Infected, compound **5** treated group (received 100 μL of compound **5** at a dose of 12.5
172 mg/kg/day for 7 days).

173 **Group VI**: Infected, pyrimethamine treated group (received 100 μL of pyrimethamine at a dose
174 of 12.5 mg/kg/day for 7 days).

175 Each mouse was intraperitoneally infected with RH strain at a dose of 2500 tachyzoites/100 μL
176 except the healthy control group. All the tested drug doses were fixed as described for the control
177 known drug pyrimethamine (12.5 mg/kg/day for 7 days) according to Romand et al. [27]; Jiang
178 et al. [28] and Jafari et al. [29].

179 **Evaluation of the treatment efficacy:**

180 **2.2.2.1. Parasitological study**

181 **2.2.2.1.1. Survival time**

182 Survival time was assessed daily for each assigned group for 30 days and Kaplan-Meier survival
183 curve was used to determine the percentage of mice living over time [30].

184 **2.2.2.1.2. Estimation of the parasite count**

185 On day 8, mice were anesthetized and sacrificed by cervical dislocation. Peritoneal exudate,
186 liver, spleen, and brain tissue were collected from all assigned groups to assess the tachyzoites
187 count. A thin smear was prepared from each sample, fixed with methanol, then dried and stained
188 with Giemsa stain for 10 min. After staining the prepared slides were washed with tap water drop
189 wisely. 10 different fields were examined using light microscope (oil immersion lens) to measure

190   the mean parasite count in each subgroup (ten fields/each slide and three slides/each organ) [31,

191   32]. Then parasite percent reduction (%R) was calculated through the following formula:

$$\%R \ = \frac{C - E}{C} \times 100$$

192

193   Where %R represents percent reduction, C represents the number of tachyzoites in the control

194   group (untreated group), and E represents the number of tachyzoites in the study group of mice

195   [33].

196   **2.2.2.1.3. Morphological study of tachyzoites of *T. gondii***

197   On day 8, the peritoneal fluid of all infected treated subgroups was collected, followed by

198   fixation in glutaraldehyde, then prepared for scanning electron microscope (SEM) examination

199   of the tachyzoites' ultrastructure [34].

200   *2.3. Histopathological study*

201   Liver, spleen, and brain tissues were taken from each mouse at the end of the study, followed by

202   fixation step in 10% formalin, paraffinized, sectioned, then stained with hematoxylin-eosin

203   (H&E), and finally examined by light microscopy for possible histopathological changes [34].

204   *2.4. Statistical analysis*

205   The data was displayed as mean SD. SPSS version 20 was used to analyze the data. The

206   ANOVA F-test was employed to calculate the difference in numerical variables between groups.

207   **3. Results and discussion**

208   *3.1. Chemistry*

209   Ionic liquids are usually prepared by quaternization of nitrogen-containing molecules. In this

210   study, the focused 1,2-di(pyridin-4-yl)ethane (**1**) was selected as the starting reactant for the

211   production of the desired bis-ionic liquids (bis-ILs), as shown in **Scheme 1**. Thereby, the two

212   pyridine nitrogen atoms of the dipyridylethane (**1**) were bis-alkylated with two equivalents

213   of benzyl bromide in refluxing acetonitrile, yielding the bis-benzyl pyridinium bromide

214   in high yield (94%) (Scheme 1).

215
216
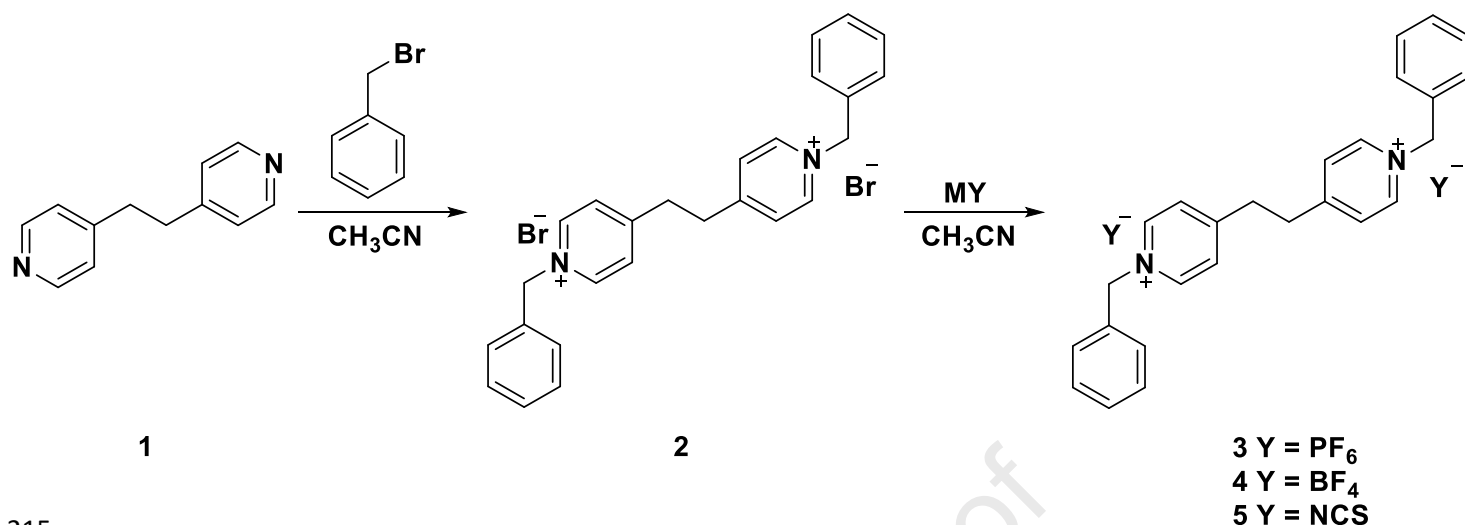
217   **Scheme 1:** Synthesis of bis-benzyl pyridinium based-ionic liquids **2-5.**

218   The ^{1}H and ^{13}C NMR data of compound **2** supported the accomplishment of this

219   quaternization procedure. Therefore, the proton NMR spectrum showed the appearance of two

220   distinct singlets at δ_H 5.83 and 3.23 ppm of 1:1 ratio that can be assigned to the benzylic NC**H$_2$**

221   and C**H$_2$**CH$_2$ protons, respectively. The carbon signals belonging to the same groups NCH$_2$Ph

222   and C**H$_2$**CH$_2$ resonated in its ^{13}C NMR spectrum at 62.83 and 34.28 ppm, respectively (See

223   experimental section). These results confirmed the presence of two benzyl groups in its structure.

224   The bis-pyridinium ionic liquid bromide **2** was then metathetically treated to displace the

225   two bromide atoms and insert new counter anions (PF$_6^-$, BF$_4^-$, NCS$^-$). In this regard, thermal

226   treatment of bis-ILs **2**, in acetonitrile for 24 hours, with various metal salts afforded the

227   corresponding bis-pyridinium ionic derivatives **3-5** tethering such desired counter anions in 90-

228   92% yields.

229   The metathesis reaction was successful, as evidenced by spectroscopic analysis of the

230   resulting ILs **3-5**. However, their ^{1}H and ^{13}C NMR spectra did not differ from those of the

231   corresponding bromide analogue **2**.

232   The incorporation of two PF$_6^-$ anions on the structure of derivative **3** was thus proved by

233   the investigation of the ^{31}P and ^{19}F NMR spectra. The ^{19}F NMR spectrum (Figure 1) disclosed

234   one distinct doublet at -69.25 ppm, whereas the ^{31}P spectrum (Figure 2) has been characterized

235   by one septet between -131.01 to -157.36 ppm.

236   The presence of one distinct doublet at -69.25 ppm was detected in the ^{19}F NMR
237 spectrum (Figure 1), whereas one septet was detected in the ^{31}P spectrum between -131.01 to
238 -157.36 ppm (Figure 2).
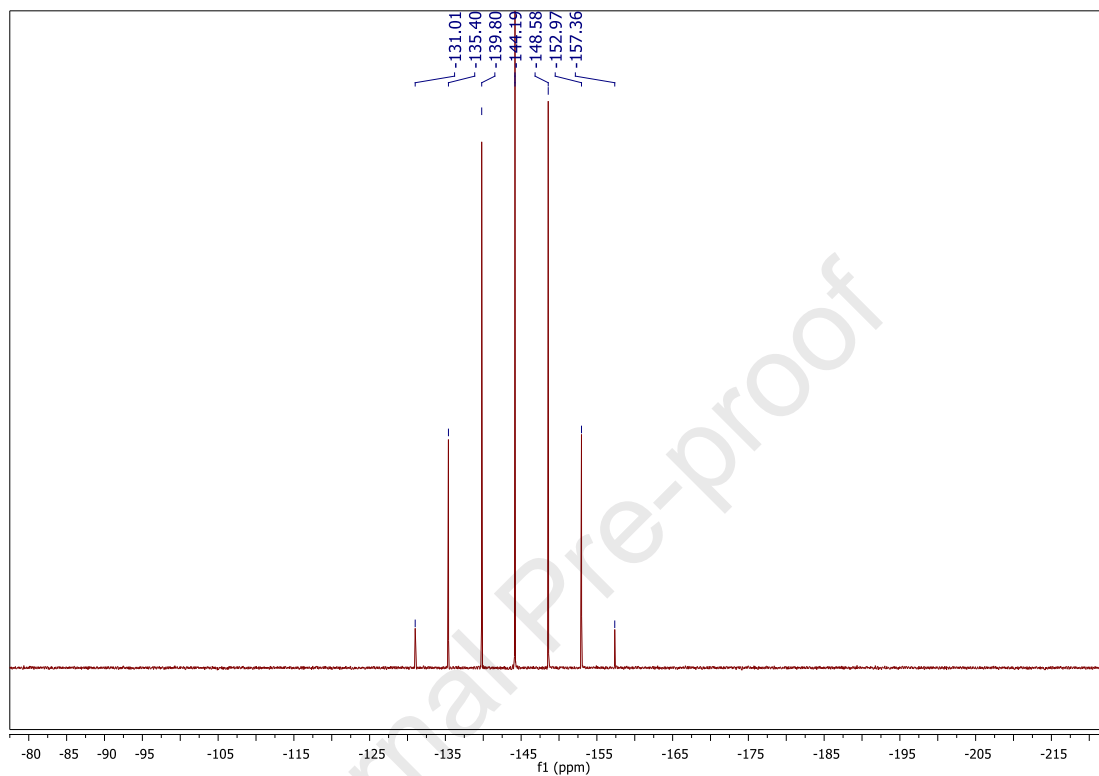
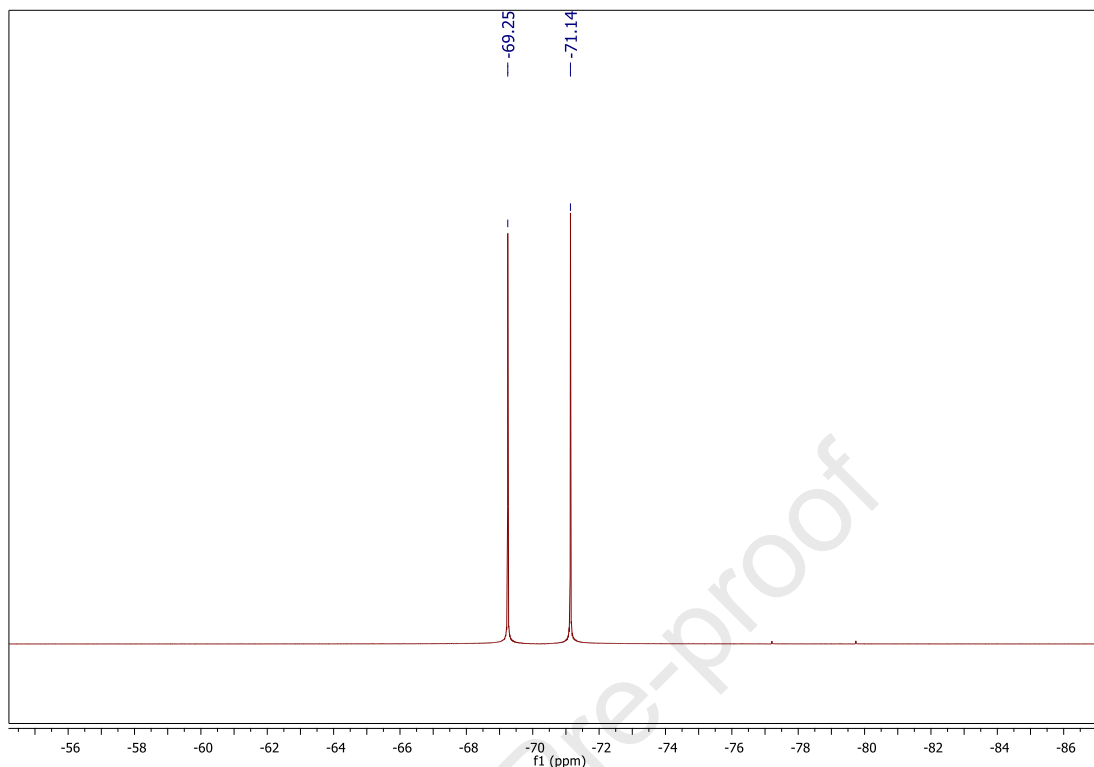**Figure 1**: ^{31}P-NMR spectrum of compound **3**.

241

242 **Figure 2**: ^{19}F-NMR spectrum of compound **3**.

243   The ^{11}B NMR and ^{19}F NMR analysis of the resulted di-pyridinium **4** facilitated the

244 confirmation of the tetrafluroborate (BF$_4^-$) anion exchange. The boron spectrum (Figure 3)

245 showed a characteristic multiplot between -1.28 to -1.30 ppm, and the ^{19}F NMR spectrum

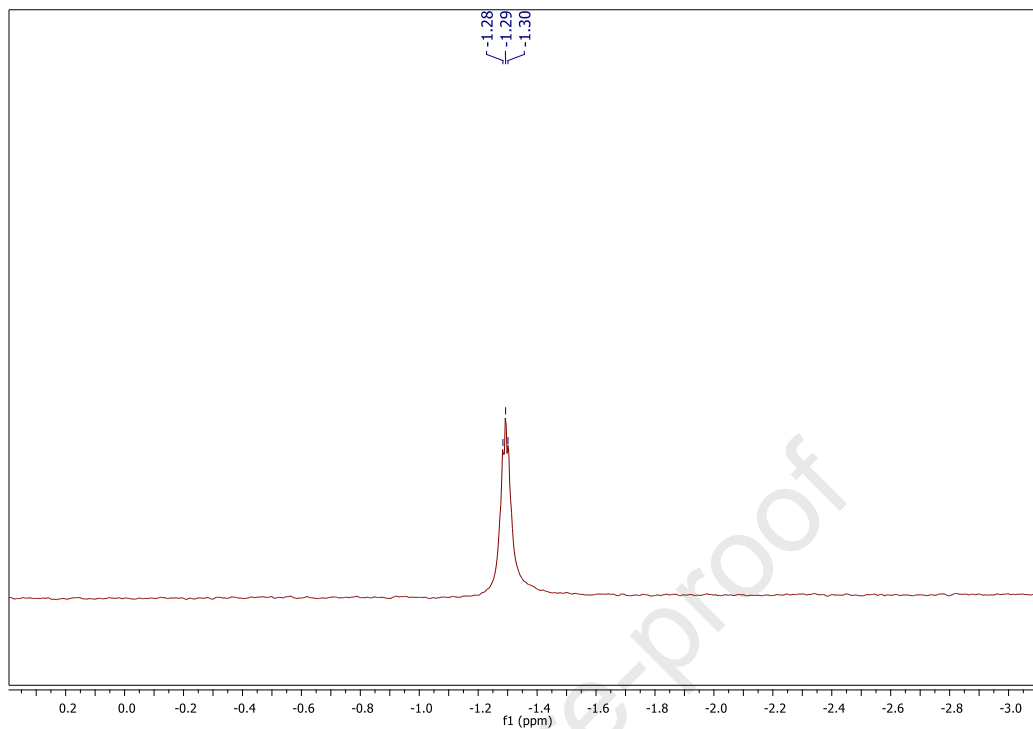246 (Figure 4) displayed two doublets at -148.24 and -148.30 ppm.

247

-1.28
-1.29
-1.30

f1 (ppm)

Figure 3: ^{11}B-NMR spectrum of compound **4**.

249

-148.24
-148.25
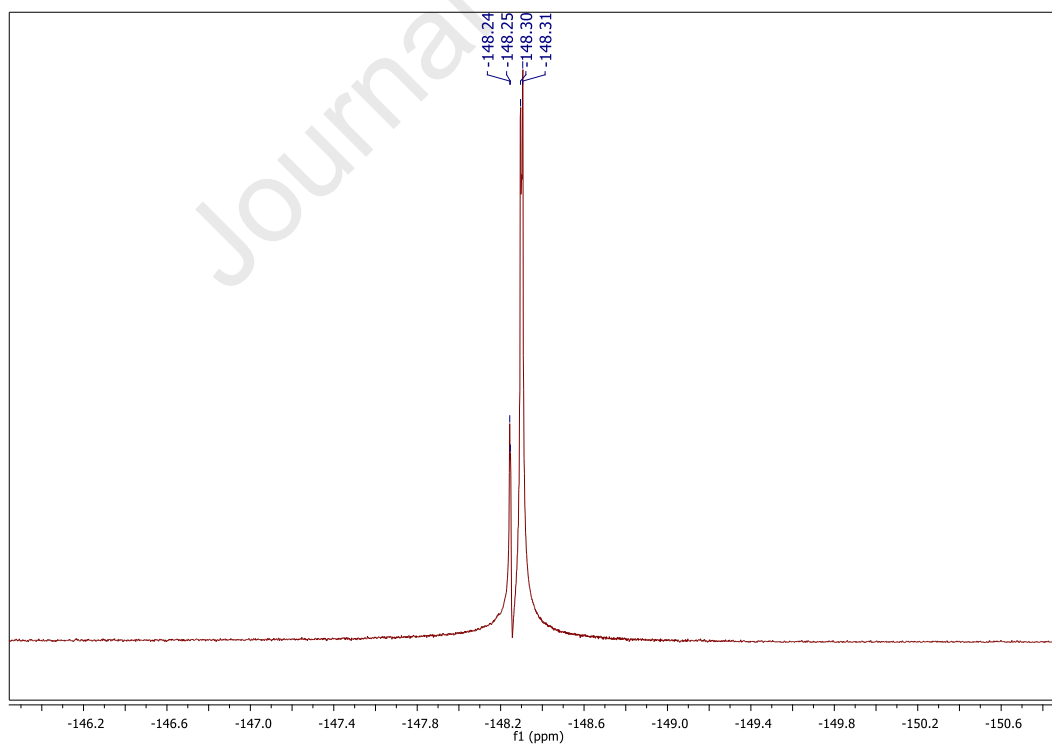-148.30
-148.31

f1 (ppm)

Figure 4: ^{19}F-NMR spectrum of compound **4**.

251   In contrast to compounds **3** and **4**, IR spectroscopy proved to be very useful in confirming

252 the formation of di-cationic ionic liquid **5** with thiocyanate (NCS⁻) as counter anions due to the

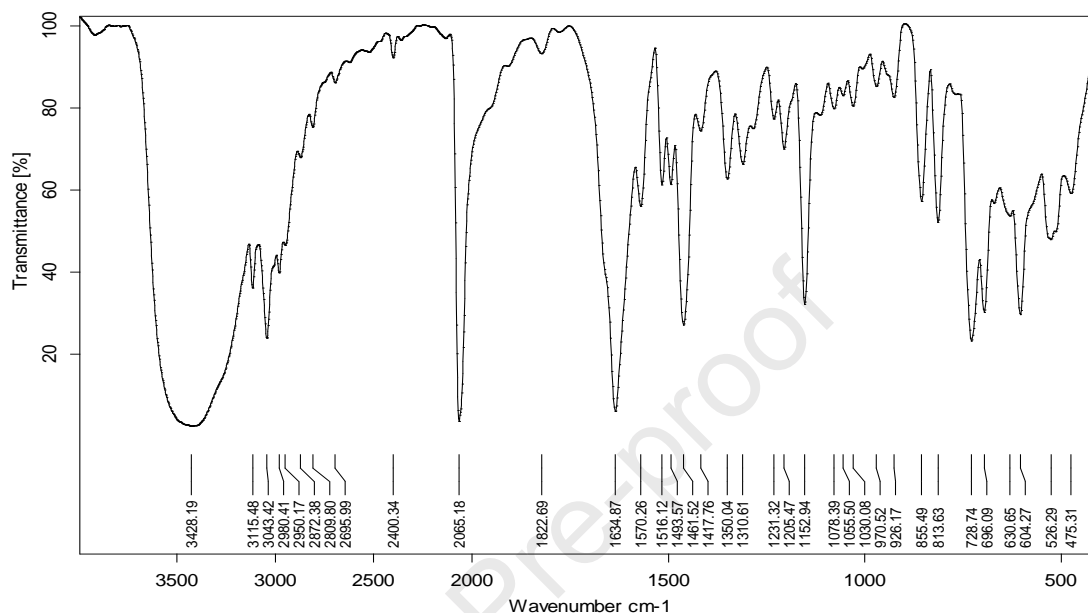253 appearance of a strong absorption band at 2065 cm^{-1} attributed to such an anion (Figure 5).

254

255   **Figure 5**: IR spectrum of compound **5**.

256 *3.2. Cytotoxicity study*

257 The in vitro cytotoxic effect of the synthesized compounds was evaluated in HepG2 cell line. It

258 was revealed that at 500 μg/mL of the tested compounds 3, 4 and 5, the normal liver cell

259 viability% was 19.4, 30.1 and 37.14% respectively (Figure 6). Moreover, data revealed that

260 compound 5 showed the highest cell viability% among the tested compounds with CC_{50} reached
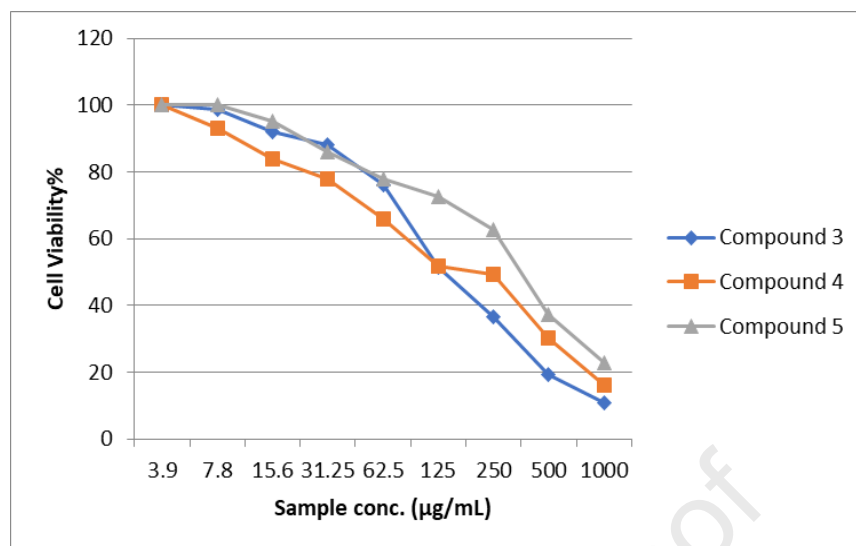
261 375 μg/mL.

262

263 **Figure 6:** Cytotoxic effect of the synthesized compounds.

3.3. Antiparasitic activity

264

265 *3.3.1. Survival rate*

266 The survival rate was studied among the assigned groups for 30 days and data revealed that
267 Group I (healthy uninfected mice) showed the highest mean survival time compared to infected
268 groups. It was noticed that among the infected treated groups, Group V and VI showed the
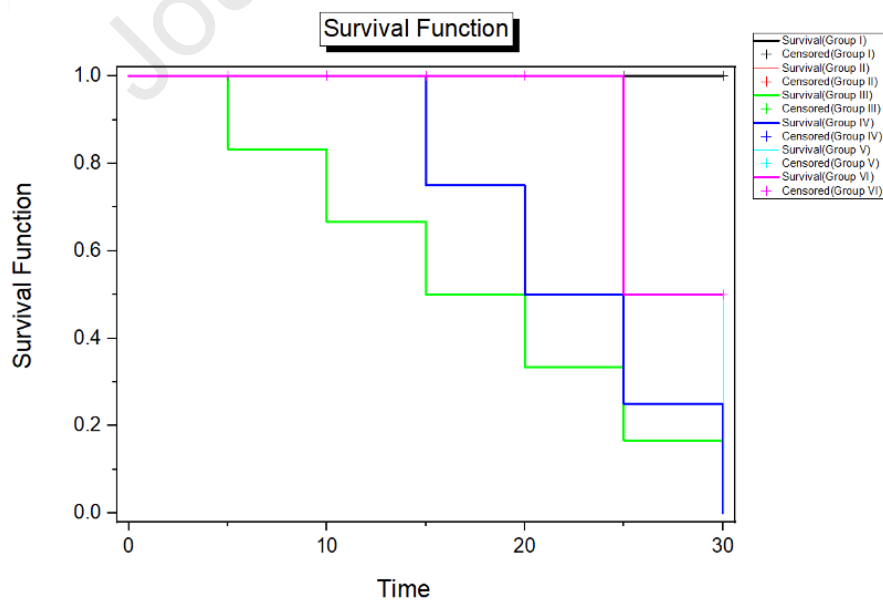269 highest survival time (Figure 7).

270

271 **Figure 7:** Kaplan-Meier overall survival curve of the tested groups.

272 *3.3.2. Parasite count and percent reduction (%R)*

273 Mean tachyzoite counts were significantly high in all the experimental groups in relation to the

274 liver impression smears compared to other organs with %R reached 38, 50, 77 and 79 for groups

275 III, IV, V and VI respectively with statistically significant differences with untreated infected

276 group (group II).

277 Statistically significant reductions in tachyzoites count and the highest rate of reduction among

278 the treated mice was recorded in groups **V** and **VI** in all organs compared to untreated infected

279 group. However, there was no statistically significant difference between these two groups

280 (group V and VI) (Table 1, Figure 8 (1-3))

281 Di-cationic and similar compounds that use amidine groups as the source of the cationic moiety

282 have been tested for their antimicrobial effects and their actions against a variety of human

283 pathogens, including *Toxoplasma gondii*, which may approve our findings [35]. Furthermore, a

284 previous study that aimed to evaluate the rate of growth of *T. gondii* tachyzoites in Human

285 Foreskin Fibroblast (HFF) cell line using two in vitro techniques revealed that 2-pyridine bearing

286 5-substituted 4-thiazolidinone and 2-pyridinyl hydrazinyl derivatives, exhibited the best anti-*T.*

287 *gondii* activities with low cytotoxicity [36]. Moreover, Hopper *et al*. [37] discovered that 5- (4-

288 (3-(2-methoxypyrimidin-5-yl)phenyl)piperazin-1-yl)pyrimidine-2,4-diamine   was   extremely

289 effective in regulating the active infection of the hypervirulent strain of *T. gondii* in the murine

290 model.

291 **Table 1:** Number and rate of reduction of parasites in organs of RH-infected mice.

	Liver (n=10)	Spleen (n=10)	Brain (n=10)
Group II[a] **Mean ± SD**	14.9± 1.45[b,c,d,e]	8.9±1.37[b,c,d,e]	1.4 ± 0.66[c, e]
Group III (IL 2)[b] **Mean ± SD** **R%**	9.3 ± 1.95[a,c,d,e] 38	7.2 ± 1.32[a,c,d,e] 19	1.1±0.54[c,e] 21

Group IV(IL 3)[c] **Mean ± SD** **R%**	$7.4\pm 1.78^{a,b,c,e}$ 50	$5.4\pm 0.97^{a,b,c,e}$ 39	0.8 ± 0.60^{e} 43
Group V (IL 5)[d] **Mean ± SD** **R%**	$3.5\pm0.53^{a,b,d}$ 77	$2.8\pm0.63^{a,b,d}$ 69	$0.3\pm0.46^{a,b}$ 79
Group VI(pyrimethamine)[e] **Mean ± SD** **R4%**	$3.2\pm 0.79^{a,b,d}$ 79	$2.5\pm0.71^{a,b,d}$ 72	$0.2\pm0.40^{a,b,d}$ 86
F ***p***	116.11 < 0.001	70.37 < 0.001	8.11 < 0.001

292   **n**: The number of mice in the subgroup; **SD**: standard deviation, F: F test (ANOVA) and $p \leq 0.05$(statistically
293   significant). [a]Significant with subgroup **II**; [b]Significant with subgroup **III**; [c]Significant with subgroup **IV**;
294   [d]Significant with subgroup **V**; [e]Significant with subgroup **VI**.
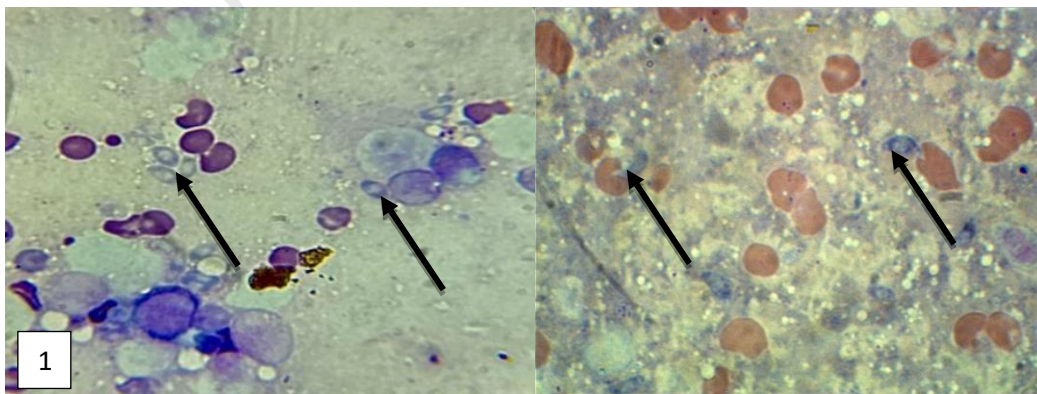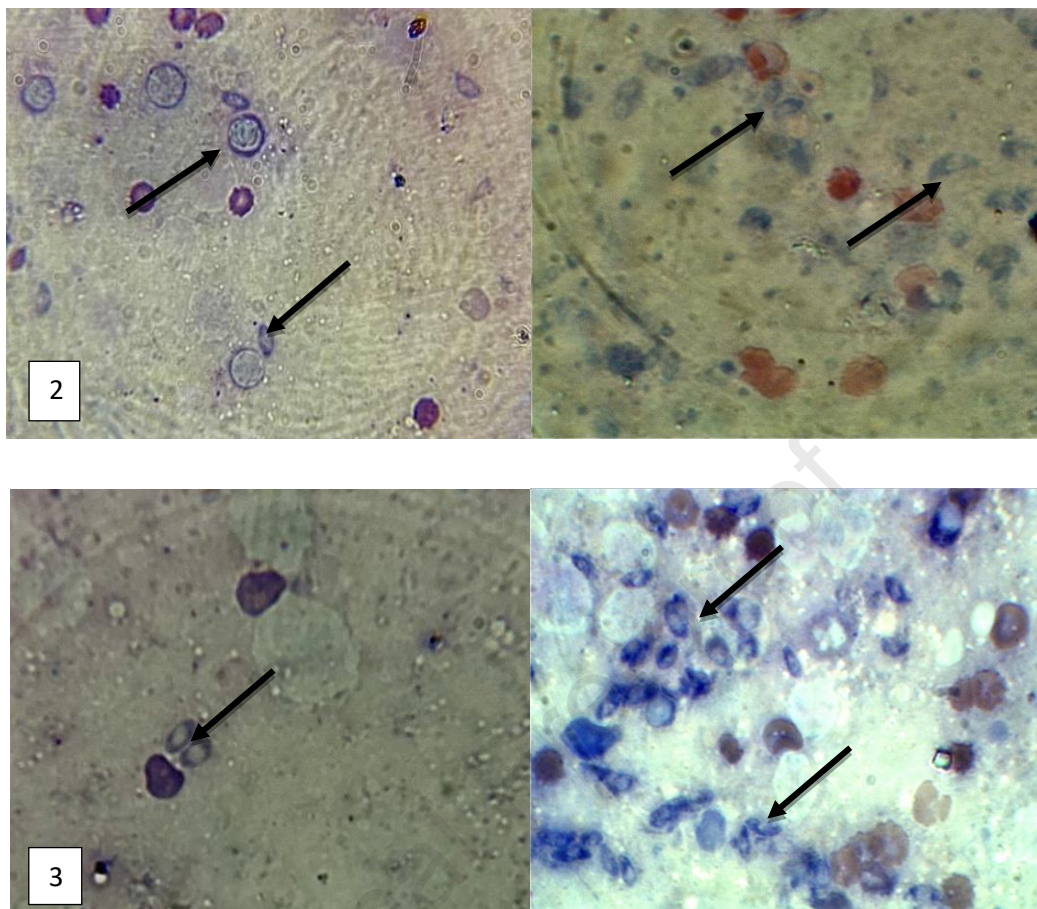
Figure 8: Tachyzoites of *T. gondii* of infected mice which received compound **5** in Giemsa-stained liver tissue (**1**), Spleen (**2**) and brain (**3**) impression smears, X 1000.

Scanning electron microscope study of the control group (II) revealed a normal smooth surface of *T. gondii* tachyzoites while SEM analysis of group V peritoneal fluid showed distortion and deformation in tachyzoites' shape (Figure 9 (A-C)).
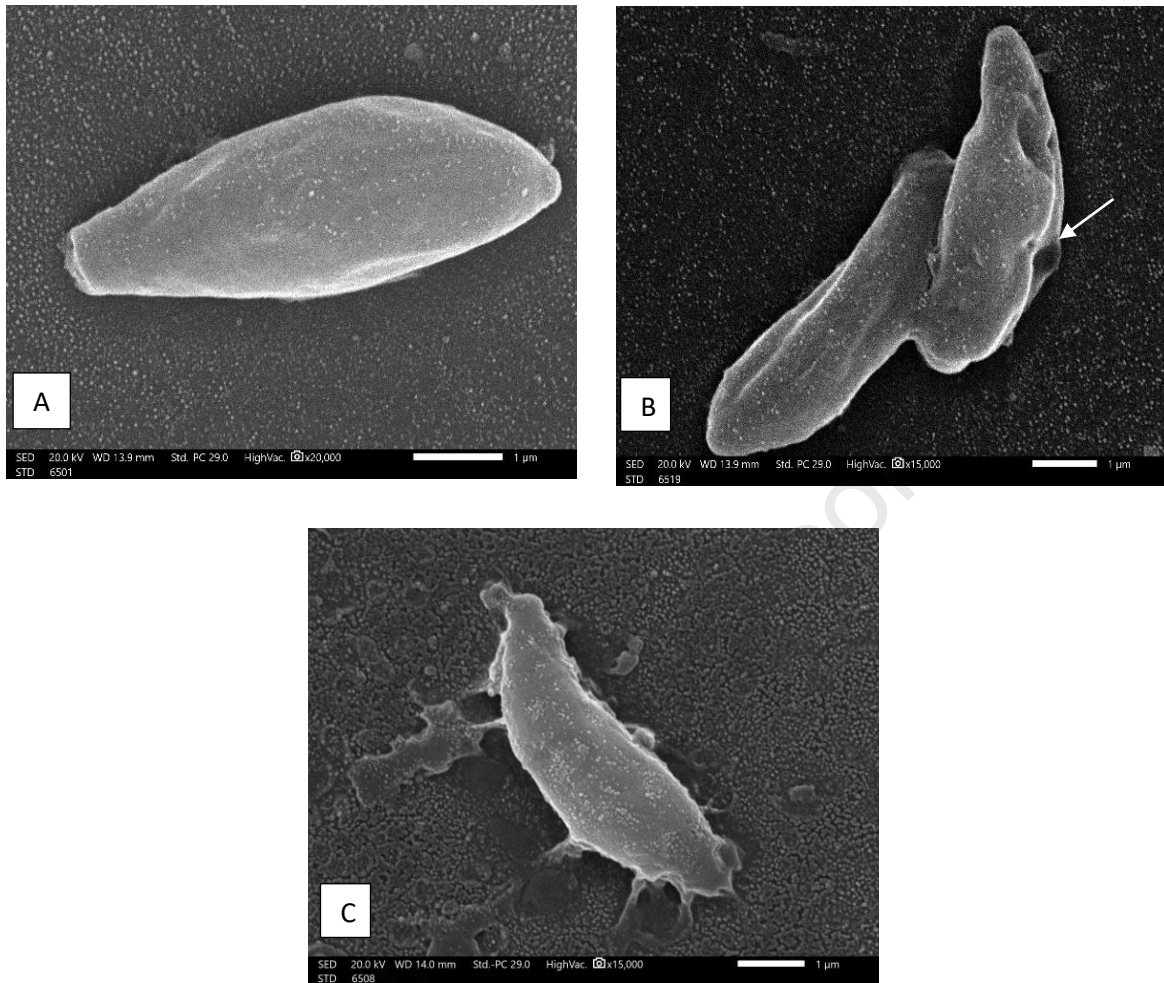
Figure 9: SEM photo of tachyzoite of *Toxoplasma gondii* in infected unreeled drug group showing regular smooth surface and evident conoid (x 20,000) (**A**) while (**B, C**) showing *Toxoplasma gondii* tachyzoite in group V which shows irregular, ridge surface and irregular papules and dimples (arrow) (x 15,000).

3.4. Histopathological study

3.4.1. Liver

The findings indicate normal cytoarchitecture of hepatocytes going to extend from the central vein, which was confirmed by plate 1 of the control group and groups **III** and **VI** illustrating treatment effectiveness in contrast to antibiotic effects. A clogged, dilated central vein was also seen in the negative control group.

310   Furthermore, in groups, normal cells in the Center had polyhedral shape, vacuolated acidophilic

311   cytoplasm, and rounded vesicular nuclei (1, 3, and 6). The tested compound **2** group has

312   increased vacuolation, indicating that therapy had the least effect on those hepatocytes. Hepatic

313   sinusoids were observed to be tiny spaces surrounded by flattened endothelial cells. In way of

314   comparison to this description, the negative control group, groups **IV**, **V**, and **VI** showed

315   congestion of blood sinusoids, with group **V** showing a decrease in congestion, indicating that

316   the investigated derivative **5** had a greater effect on liver tissue. Normal scattered irregular

317   kupffer cells with oval nuclei between the hepatic cords in all groups.

318   Early apoptotic symptoms including such hazy vacuolated cytoplasm and imprecise cell borders

319   were noticed in the negative control group. Nuclear alterations include nuclear division, nuclear

320   eccentricity, and pyknosis, as well as necrosis. Furthermore, cellular infiltrate was present in this

321   group, but at a lower ratio than in the derivative **2** in the four groups (Figure 10 (Liver A-F)).

322   *3.4.2. Spleen*

323   The structure of the spleen in the control group was characterized by well-defined white and red

324   pulp with continuous trabeculae through all tissues encountered by the capsule. The whitish pulp

325   contained lymphoid follicles as well. With the presence of trabeculae, Groups **III & VI** provided

326   a similar definition. White pulp also has a consistent marginal zone and core.

327   The negative control group had the most splenic tissue damage, as evidenced by disordered

328   white and red pulp and the presence of tachyzoites. The compound **2** group exhibited large,

329   blocked blood arteries. Furthermore, the limits between white pulp and red pulp regions were not

330   noticed, which was critical to the lowest extent of this treatment on splenic tissue.

331   Increase in the number of lymphoid follicles in the compound **4** group, underlining the

332   importance of this therapy at this phase with the identification of the capsule around the spleen.

333   In comparison to earlier studies, the alienated structure of group **VI** reflects the efficacy of the

334   investigated compound **5** to the splenic tissue in similar action of antibiotic treatment.

335   The compound **5** group had to have an increase in lymphoid follicles, highlighting the

336   significance of this treatment at this stage with the identification of the capsule around the

337   spleen. In comparison to previous studies, the alienated configuration of group **VI** tends to reflect

338   the efficacy of the derivative **5** to splenic tissue in an antibiotic-like action (Figure 10 (Spleen A-

339   F)).

340   *3.4.3. Brain*

341   Microscopic examination of H & E-stained cerebral cortex slices from the frontal region of the

342   control group revealed the well-known normal cytoarchitecture of the cerebral cortex. Neurons,

343   particularly pyramidal and granule cells, as well as neuroglial cells, are abundant within these

344   layers. Significant multifocal histological abnormalities, culminating in a massive cerebral

345   infract, were found when the infected group was examined.

346   In comparison to the previous findings, the treated groups (**IV** & **V**) had better histology and

347   fewer vacuoles and small-disconnected brain foci. Besides that, tachyzoites were detected in

348   group **IV**. Normal neuron architecture, with large vesicular nuclei in the center with one or more

349   nucleoli and peripheral dispersion of Nissl granules were recorded indicating the influence of the

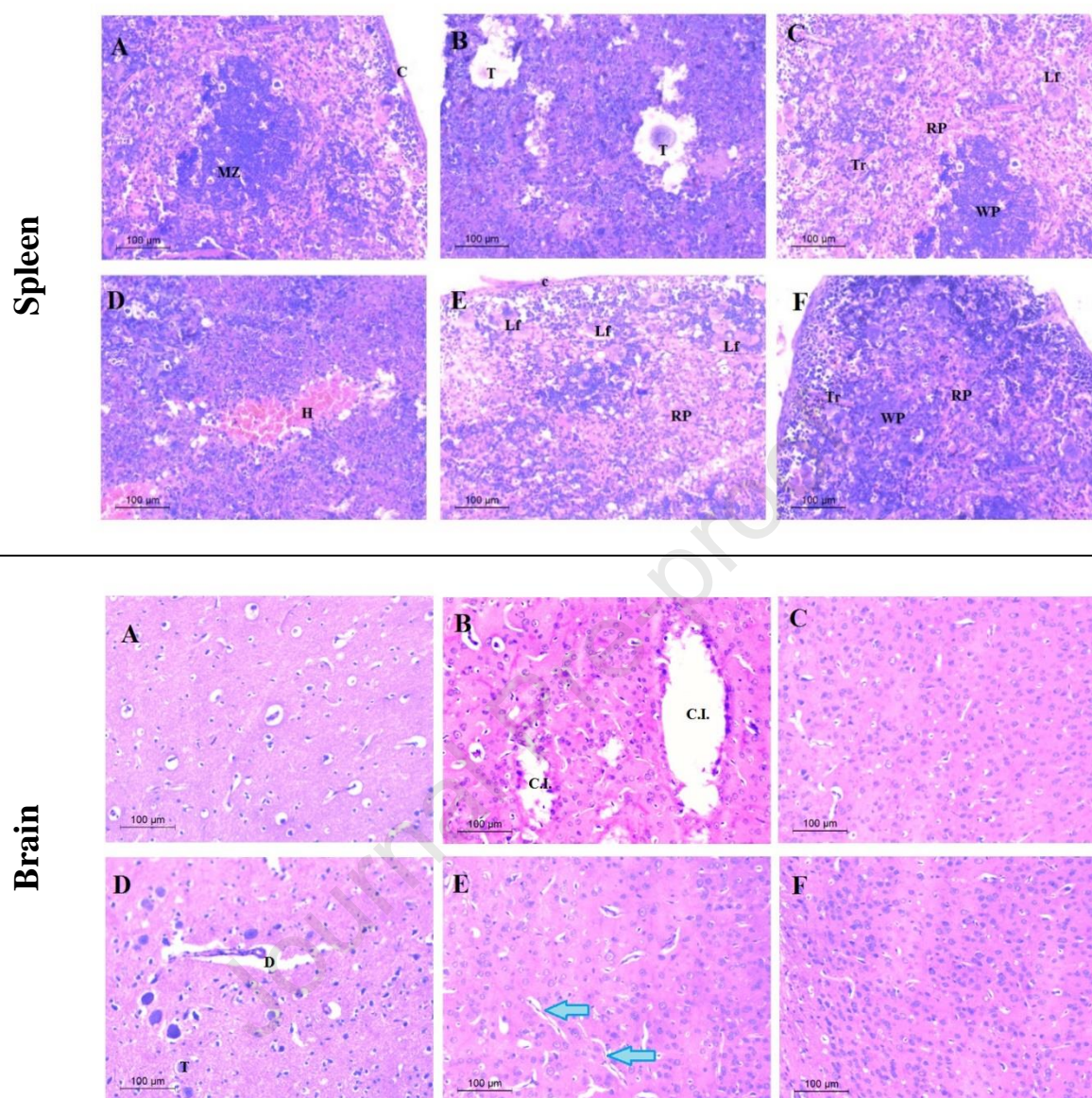350   ionic liquid **5** treatment versus antibiotic treatment (Figure 10 (Brain A-F)).

351
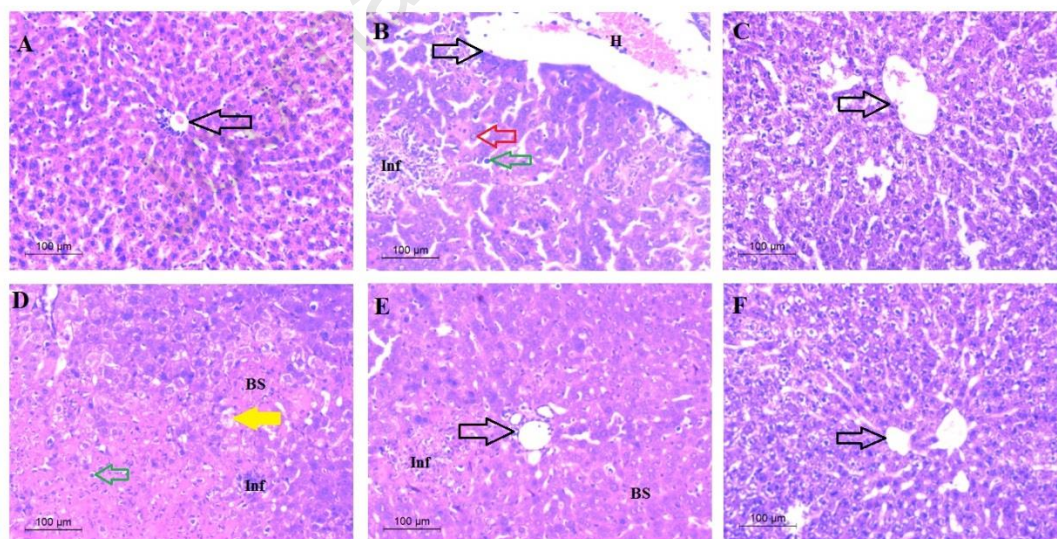
Liver

Figure 10: A photomicrograph illustrates several H&E-stained tissue specimens from the liver spleen, and cerebrum. (**A**): control group; (**B**): infected group; (**C**): antibiotic Treated group; (**D**): compound **2** treated group; (**E**): compound **5** treated group; (**F**): compound **3** treated group magnification X 100. Where Black arrows central vein, Yellow arrow vacuolated hepatocyte, Inf cellular infiltrate, BS blood sinusoids, H hemorrhage, Green arrows Kupffer cells, T tachyzoites, MZ marginal zone, RP red Pulp, C capsule, Tr trabeculae, WP white pulp, L lymphoid follicle, C.I. cerebral infract, D degeneration, Blue arrow irregular body of neurons.

360 **Conclusion**

361 Focused bis-pyridinium based-ionic liquids were successfully synthesized through the
362 quaternization of the selected 1,2-di(pyridin-4-yl)ethane followed by metathetical anion
363 exchange. The synthesized pyridinium derivatives were fully characterized using various NMR-
364 spectroscopic techniques including ^{1}H, ^{13}C, ^{11}B, ^{31}P and ^{19}F-NMR. The current available
365 treatments for *Toxoplasma gondii* infection are restricted, besides that possess side effects and
366 the spread of drug-resistant *T. gondii* strains. Consequently, a new anti-*Toxoplasma* drug should
367 be available, therefore we emphasized novel alternatives, and well tolerated compounds. The
368 investigated dicationic pyridinium derivatives exhibited a great reduction in *T. gondii* tachyzoites
369 count in various organs compared to pyrimethamine (the known available drugs for
370 toxoplasmosis). However, more drug doses need to be tested with further molecular and
371 immunological studies are needed before testing the synthesized drugs in clinical studies.

372

373

374 Author contribution statement:

375

376 Esraa Abdelhamid Moneer, Basant A. Bakr, Sara H. Akl, Yahya H.
377 Shahin, Bassma H. Elwakil, Mohamed Hagar, Keshav Raj Paudel,
378 Ateyatallah Aljuhani, Mohamed Reda Aouad; Nadjet Rezki:
379 Conceived and designed the

380 experiments; Performed the experiments; Analyzed and interpreted
381 the data; Contributed reagents, materials, analysis tools or data; Wrote
382 the paper. </p>

383

384 Funding statement:

385

388

389   Data availability statement:

390

391   Data will be made available on request.

392

393   Declaration of interest's statement:

394

395   The authors declare no competing interests.

396

397   Additional information:

398

399   Supplementary content related to this article has been published online at [URL].

400

401

402

403   **Declarations**

404   **Author contribution statement**

405   Esraa Abdelhamid Moneer, Basant A. Bakr, Sara H. Akl, Yahya H. Shahin, Bassma H. Elwakil,

406   Mohamed Hagar, Keshav Raj Paudel, Ateyatallah Aljuhani, Mohamed Reda Aouad; Nadjet

407   Rezki: Conceived and designed the experiments; Performed the experiments; Analyzed and

408   interpreted the data; Contributed reagents, materials, analysis tools or data; Wrote the paper.

409   **Funding statement**

410   This work didn't receive any external fundings.

411   **Data availability statement**

412   Data included in article/supp. material/referenced in article.

Declaration of interest's statement

The authors declare no conflict of interest.

References

1. Lei Z., B. Chen, Y.-M. Koo, D.R. MacFarlane, ACS Publications, 2017, p. 6633-6635.

2. Singh S.K., A.W. Savoy, Journal of Molecular Liquids 297 (2020) 112038.

3. Singh R., A. Rasool, Br J Res 6 (2018) 45.

4. Egorova K.S., E.G. Gordeev, V.P. Ananikov, Chemical Reviews 117 (2017) 7132.

5. Gomes J.M., S.S. Silva, R.L. Reis, Chemical Society Reviews 48 (2019) 4317.

6. Ding, M. Zha Y.-S., J. Zhang, S.-S. Wang, Colloids and Surfaces A: Physicochemical and Engineering Aspects 298 (2007) 201.

7. Steudte S., S. Bemowsky, M. Mahrova, U. Bottin-Weber, E. Tojo-Suarez, P. Stepnowski, S. Stolte, 2014.

8. Payagala T., J. Huang, Z.S. Breitbach, P.S. Sharma, D.W. Armstrong, Chemistry of Materials 19 (2007) 5848.

9. Sharma P.S., T. Payagala, E. Wanigasekara, A.B. Wijeratne, J. Huang, D.W. Armstrong, Chemistry of Materials 20 (2008) 4182.

10. Balducci, A. (2018). Ionic liquids in lithium-ion batteries. *Ionic Liquids II*, 1-27.

11. Earle M.J., K.R. Seddon, Pure and applied chemistry 72 (2000) 1391.

12. Plechkova N.V., K.R. Seddon, Chemical Society Reviews 37 (2008) 123.

13. de Barros R.A.M., A.C. Torrecilhas, M.A.M. Marciano, M.L. Mazuz, V.L. Pereira-Chioccola, B. Fux, Acta Tropica (2022) 106432.

14. Oweimrin, A. (2018). Toxoplasma gondii: Antibody Prevalence and Risk Factors in CU Boulder Students.

15. Nogareda F., Y. Le Strat, I. Villena, H. De Valk, V. Goulet, Epidemiology & Infection 142 (2014) 1661.

16. Dubey J., F. Murata, C. Cerqueira-Cézar, O. Kwok, I. Villena, Parasitology 148 (2021) 1406.

17. Bogitsh, B. J., Carter, C. E., & Oeltmann, T. N. (2018). *Human parasitology*. Academic Press.

18. de Melo R.P.B., F.S. Wanderley, W.J.N. Porto, C.d.M. Pedrosa, C.M. Hamilton, M.H.G.S. de Oliveira, M. Ribeiro-Andrade, R.C.d.S. Rêgo, F. Katzer, R.A. Mota, Parasitology Research 119 (2020) 2727.

19. da Silva Sanfelice R.A., T.F. Silva, F. Tomiotto-Pellissier, B.T. da Silva Bortoleti, D. Lazarin-Bidóia, S. Scandorieiro, G. Nakazato, L.D. de Barros, J.L. Garcia, W.A. Verri, Microbes and Infection 24 (2022) 104971.

20. Anderson, A. C. (2005). Targeting DHFR in parasitic protozoa. *Drug discovery today*, *10*(2), 121-128.

21. Waller D.G., A. Sampson, A. Hitchings, Medical pharmacology and therapeutics E-Book. Elsevier Health Sciences, 2021.

22. Rezki N., M. Messali, S.A. Al-Sodies, A. Naqvi, S.K. Bardaweel, F.F. Al-blewi, M.R. Aouad, H. El Sayed, Journal of Molecular Liquids 265 (2018) 428.

23. Rezki N., S.A. Al-Sodies, H.E. Ahmed, S. Ihmaid, M. Messali, S. Ahmed, M.R. Aouad, Journal of Molecular Liquids 284 (2019) 431.

24. Al-Sodies S., N. Rezki, F.F. Albelwi, M. Messali, M.R. Aouad, S.K. Bardaweel, M. Hagar, International journal of molecular sciences 22 (2021) 10487.

25. Al-Sodies S.A., M.R. Aouad, S. Ihmaid, A. Aljuhani, M. Messali, I. Ali, N. Rezki, Journal of Molecular Structure 1207 (2020) 127756.

26. Mosmann, T. (1983). Rapid colorimetric assay for cellular growth and survival: application to proliferation and cytotoxicity assays. *Journal of immunological methods*, *65*(1-2), 55-63.

27. Romand S, Pudney M, Derouin F. In vitro and in vivo activities of the hydroxy naphthoquinone atovaquone alone or combined with pyrimethamine, sulfadiazine,

465   clarithromycin, or minocycline against Toxoplasma gondii. Antimicrob Agents
466   Chemother. 1993;37(11):2371–8.

467   28. Jiang J-H, Jin C-M, Kim Y-C, et al. Anti-toxoplasmosis effects of oleuropein isolated
468   from Fraxinus rhychophylla. Biol Pharm Bull. 2008;31(12):2273–6.

469   29. Jafari, M., Lorigooini, Z., Kheiri, S., & Naeini, K. M. (2021). Anti-Toxoplasma Effect of
470   Hydroalchohlic Extract of Terminalia chebula Retz in Cell Culture and Murine Model.
471   Iranian Journal of Parasitology, 16(4), 631.

472   30. Hagras, N. A. E., Mogahed, N. M. F. H., Sheta, E., Darwish, A. A. E., El-Hawary, M. A.,
473   Hamed, M. T., & Elwakil, B. H. (2022). The powerful synergistic effect of
474   spiramycin/propolis loaded chitosan/alginate nanoparticles on acute murine
475   toxoplasmosis. *PLOS Neglected Tropical Diseases*, *16*(3), e0010268.

476   31. Thiptara, W. Kongkaew, U. Bilmad, T. Bhumibhamon, S. Anan, Annals of the New York
477   Academy of Sciences 1081 (2006) 336.

478   32. El-Zawawy, L. A., El-Said, D., Mossallam, S. F., Ramadan, H. S., & Younis, S. S.
479   (2015). Triclosan and triclosan-loaded liposomal nanoparticles in the treatment of acute
480   experimental toxoplasmosis. *Experimental parasitology*, *149*, 54-64.

481   33. Penido M.L.d.O., D.L. Nelson, L.Q. Vieira, P.M.Z. Coelho, Memórias do Instituto
482   Oswaldo Cruz 89 (1994) 595.

483   34. Almutairi T.M., N. Rezki, M.R. Aouad, M. Hagar, B.A. Bakr, M.T. Hamed, M.K.
484   Hassen, B.H. Elwakil, E.A. Moneer, Molecules 27 (2022) 2246.

485   35. Francesconi, W.D. Wilson, F.A. Tanious, J.E. Hall, B.C. Bender, R.R. Tidwell, D.
486   McCurdy, D.W. Boykin, Journal of medicinal chemistry 42 (1999) 2260.

487   36. Molina D.A., G.A. Ramos, A. Zamora-Vélez, G.M. Gallego-López, C. Rocha-Roa, J.E.
488   Gómez-Marin, E. Cortes, International Journal for Parasitology: Drugs and Drug
489   Resistance 16 (2021) 129.

490   37. Hopper A.T., A. Brockman, A. Wise, J. Gould, J. Barks, J.B. Radke, L.D. Sibley, Y. Zou,
491   S. Thomas, Journal of medicinal chemistry 62 (2019) 1562.

Declaration of Competing Interest

The authors declare that they have no known competing financial interests or personal relationships that could have appeared to influence the work reported in this paper.